JOURNAL OF AGRICULTURAL AND FOOD CHEMISTRY

pubs.acs.org/JAFC

Article

Discovery of Pyrazine-Carboxamide-Diphenyl-Ethers as Novel Succinate Dehydrogenase Inhibitors via Fragment Recombination

Hua Li, Meng-Qi Gao, Yan Chen, Yu-Xia Wang, Xiao-Lei Zhu,* and Guang-Fu Yang*

Cite This: https://dx.doi.org/10.1021/acs.jafc.0c05646

Read Online

ACCESS | Metrics & More | Article Recommendations | Supporting Information

ABSTRACT: The discovery of novel succinate dehydrogenase inhibitors (SDHIs) has attracted great attention worldwide. Herein, a fragment recombination strategy was proposed to design new SDHIs by understanding the ligand−receptor interaction mechanism of SDHIs. Three fragments, pyrazine from pyraziflumid, diphenyl-ether from flubeneteram, and a prolonged amide linker from pydiflumetofen and fluopyram, were identified and recombined to produce a pyrazine-carboxamide-diphenyl-ether scaffold as a new SDHI. After substituent optimization, compound **6y** was successfully identified with good inhibitory activity against porcine SDH, which was about 2-fold more potent than pyraziflumid. Furthermore, compound **6y** exhibited 95% and 80% inhibitory rates against soybean gray mold and wheat powdery mildew at a dosage of 100 mg/L *in vivo* assay, respectively. The results of the present work showed that the pyrazine-carboxamide-diphenyl-ether scaffold could be used as a new starting point for the discovery of new SDHIs.

KEYWORDS: *succinate dehydrogenase, fragment, molecular docking, fungicide, diphenyl-ether*

INTRODUCTION

Succinate dehydrogenase (SDH, EC 1.3.5.1, also known as succinate-ubiquinone oxidoreductase or complex II) is one of the most important fungicidal targets and is a functional part of the tricarboxylic acid cycle and linked to the mitochondrial electron transport chain.[1,2] SDH catalyzes the oxidation of succinate to fumarate followed by reduction of ubiquinone to ubiquinol. Inhibiting SDH will cause the organism not to synthesize ATP normally and then die.[3−5] Due to its crucial role in the life cycle, 23 commercial carboxamide fungicides targeting SDH have been launched to date. Among them, the sale of pyrazole carboxamide fungicides significantly promoted market development of SDH inhibitors (SDHIs) due to high fungicidal activity and broad-spectrum properties.[6] However, according to the results from the Fungicide Resistance Action Committee (FRAC), many plant pathogens have developed resistance toward existing SDHI fungicides due to their long-term abuse and high usage rate.[7−10] Therefore, it is particularly important and urgent to design new SDHI fungicides.

Over the past several decades, some new techniques, such as high-performance computation, structure biology, and artificial intelligence, have been widely applied in structure-based drug and pesticide discovery.[11−14] Fragment-based drug discovery (FBDD) has been recognized as a successful method for hit identification and lead conception. Then, FBDD has been successfully used in many systems and yielded very promising results.[15,16] Some articles have summarized fragment-to-lead (F2L) success stories published during 2017 and 2018.[17,18] The core step in the FBDD process is to identify fragments with a low molecular weight (<300 g/mol) that weakly bind the target protein.[19] Due to the low binding affinity of fragments, they are usually difficult to detect using bioassay-based screening methods, such as high-throughput X-ray crystallography, nuclear magnetic resonance (NMR), and surface plasmon resonance (SPR).[20,21] Therefore, a variety of alternative biophysical methods have been used to detect the binding of such fragments.[22] In our laboratories, we developed a methodology for screening fragments, known as pharmacophore-linked fragment virtual screening (PFVS), which identifies high potent inhibitors for the bc_1 complex and SDH.[23,24] Recently, our group also identified potent and bioselective inhibitors for protoporphyrinogen oxidase using a fragment deconstruction method.[22] The common characteristic of PFVS and fragment deconstruction methods is fragment identification and linking. The hypothesis for fragment linking is that the binding mode of the fragments is conserved upon modification of the fragment, and when two fragments are linked together, their orientation in their respective binding district should remain the same.[22,25]

In this study, we report the molecular design of new SDHIs using a fragment identification and recombination strategy, which includes five steps: (1) to uncover the ligand−receptor interaction mechanisms of four representative SDHIs, including pyraziflumid, flubeneteram, pydiflumetofen, and fluopyram (Figure 1), by integrating molecular docking, molecular dynamics, and binding energy calculations; (2) to identify three active fragments, pyrazine from pyraziflumid, diphenyl-ether from flubeneteram, and prolong amide linker from pydiflumetofen and fluopyram, which occupied three different sub-pockets in the SDH binding site; (3) to combine three active fragments and produce four virtual compounds

Received: September 1, 2020
Revised: October 29, 2020
Accepted: November 4, 2020

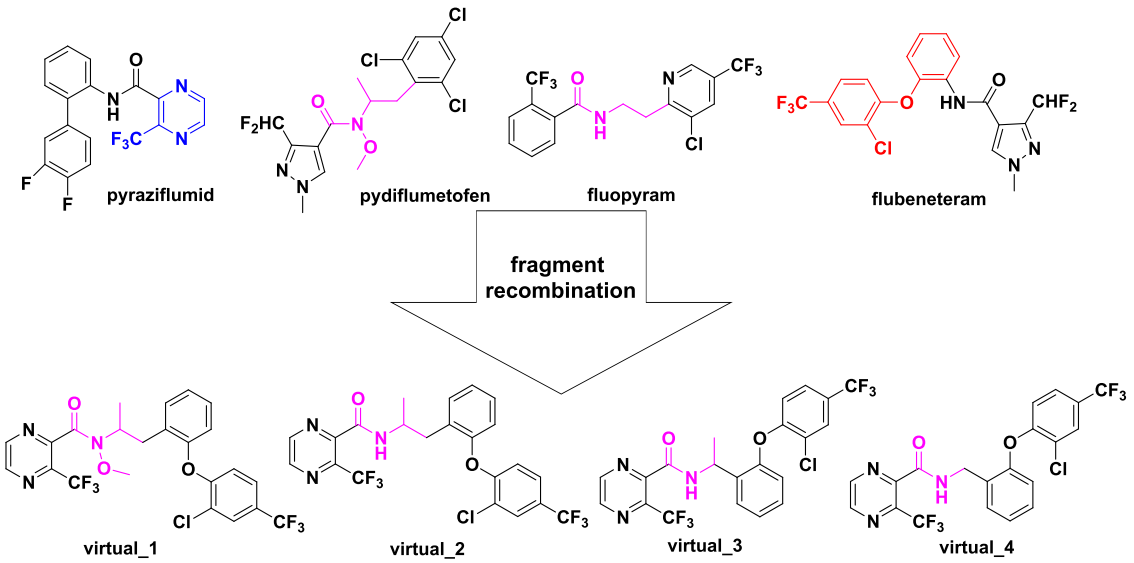

Figure 1. Design of virtual compounds. Pyraziflumid, pydiflumetofen, and fluopyram are commercial SDH fungicides. Flubeneteram is a candidate SDH fungicide and is not currently on the market. Virtual-1, virtual-2, virtual-3, and virtual-4 were designed based on the above compounds with different amine bond lengths.

(virtual-1, virtual-2, virtual-3, and virtual-4); (4) to synthesize a series of pyrazine-carboxamide-diphenyl-ether scaffold based on virtual-3 and virtual-4 binding modes and evaluate their structural−activity relationship *in vitro* and *in vivo*; and (5) one hit compound **6y** was identified with an IC_{50} value of 0.83 μM against porcine SDH, which was about 2-fold more potent than pyraziflumid (IC_{50} = 1.52 μM). Further biological assays showed that compound **6y** had excellent fungicidal potency toward *Botryotinia fuckeliana in vitro* and soybean gray mold *in vivo*. Computational simulations revealed that compared to the commercial fungicide pyraziflumid, compound **6y** showed a more favorable VDW interaction with SDH, which led to its higher activity. The present study provides an example of an application of computational design of pesticide molecules.

MATERIALS AND METHODS

Chemistry. All reagents and solvents were commercially available and used directly without further purification. Reactions were monitored by thin-layer chromatography (TLC). Target compounds were purified by column chromatography using silica. The ^{1}H NMR (600, 500, or 400 MHz) and ^{13}C NMR (125 MHz) spectra were recorded on a Bruker Avance 500 spectrometer (Bruker Inc., Billerica, MA), Mercury Plus 400 MHz, or 600 MHz spectrometer (Varian, Palo Alto, CA) in DMSO-d_6 or $CDCl_3$ solution, with $SiMe_4$ (TMS) as the internal standard. Mass spectrometry (MS) data were obtained with a DSQII GC−MS (Thermo Fisher, Austin, TX) instrument with an electrospray ionization (ESI) source. High-resolution mass spectra (HRMS) were determined with an Agilent 6224 time-of-flight liquid chromatograph mass spectrometer (Agilent Technologies, Santa Clara, CA), which was equipped with a 250 mm × 4.6 mm i.d., 5 μm, Eclipse XDB-C18 (Agilent Technologies, Santa Clara, CA) column. The melting points were determined on a BüCHI B-545 melting point apparatus and were uncorrected. Detailed synthetic routes and characterization data for all synthesized compounds are given in the Supporting Information.

Molecular Model. The 3D structures of the newly synthesized compounds were built using SYBYL and then minimized with the steepest descent method and conjugate gradient method, both with 2000 steps with a convergence criterion of 0.001 kcal/mol/Å.[26] The crystal structure of porcine SDH (PDB ID: 1ZOY)[2] was chosen as the receptor.

Molecular docking was performed using Autodock4.2.[27] The grid center was set according to the UBIQUINONE ligand in 1ZOY. The grid box was set as 42 × 34 × 50, and the grid space was set at 0.375 Å. The default values were used for all other parameters. The 256 conformations were acquired with the conformation search method of the Lamarckian Genetic Algorithm (LGA)[27] and then subjected to further energy minimization and short molecular dynamics (MD) simulation using Amber16.[28,29] First, the ligand was minimized with the protein fixed. Second, only the backbone atoms of the protein were fixed. Last, minimization was carried out with all the atoms without any constraint. Each step of minimization was performed by means of 1000 cycle steepest descent and 2000 cycle conjugate gradient method, with a convergence criterion of 0.01 kcal/mol/Å. The energy minimization was followed by an additional 20 ps MD simulation, which was carried out at 300 k by applying the Langevin thermostat. The coordinate file was recorded every 1 ps. The last frame of the MD simulation was minimized with the backbone atoms of proteins fixed. Finally, the minimized complex structure was used to calculate the binding energy, making use of the molecular mechanics Possion−Boltzmann surface area (MM/PBSA) method.[24] The final structure was selected based on the binding energy and binding mode of commercial carboxamide fungicides obtained from our previous study.[30]

Enzymatic Assay. The preparation of SDH from a porcine heart was the same as previously reported.[31] The enzymatic activities of SDH were analyzed in a reaction mixture as reported previously.[32] The inhibition rates of 26 samples were measured at a 10 μM concentration. To test the IC_{50} value, reactions were carried out in the presence of varying concentrations of the inhibitor.[33,34] The commercial fungicide pyraziflumid was chosen as a positive control.

***In Vitro* Fungicidal Activity.** Compounds were evaluated in mycelia growth inhibition tests against *Phytophthora capsici*, *Pythium dissimile*, *B. fuckeliana*, *Gibberella zeae*, and *Zymoseptoria tritici* (rich media) in artificial media and *Uromyces viciae-fabae* on bean leaf disks.[35] All testing was done by Syngenta AG and undertaken on 96-well microtiter plates. Each testing was carried out in triplicate.[36] Three commercial fungicides were chosen as positive controls.

***In Vivo* Fungicidal Activity.** According to the published pesticide bioassay testing method in Shenyang Sinochem Agrochemicals R&D Co., Ltd. (Shenyang, China),[37] 13 target compounds were evaluated for protective activities in the greenhouse against wheat powdery mildew and soybean gray mold. The commercial fungicide pyraziflumid was chosen as a positive control.

https://dx.doi.org/10.1021/acs.jafc.0c05646
J. Agric. Food Chem. XXXX, XXX, XXX−XXX

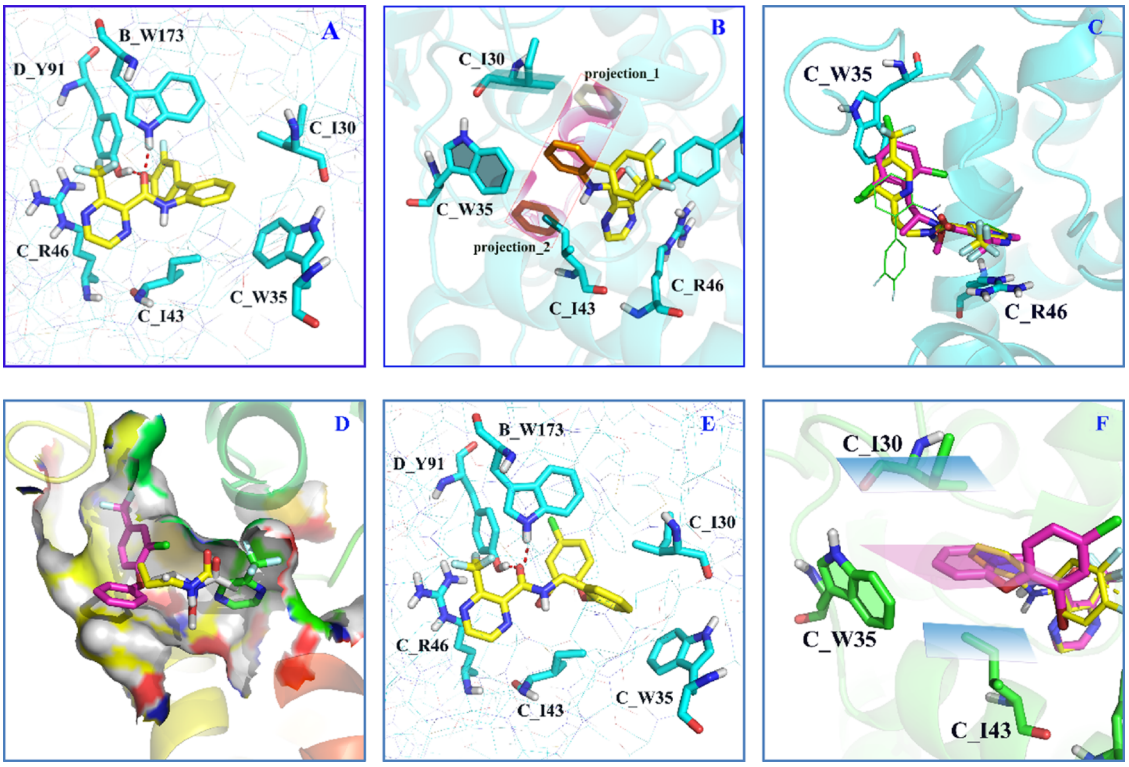

Figure 2. (A and B) Binding mode of pyraziflumid with SDH. Projection_1 and projection_2 in B are the projections of the inner phenyl in pyraziflumid. (C) Relative positions of pyraziflumid (green line), pydiflumetofen (magenta stick), and fluopyram (yellow stick) when they bound with the SDH binding site. (D) Relative positions of pyraziflumid, pydiflumetofen, fluopyram, and flubeneteram bound with the SDH binding site. For clarity, the pyrazine ring (green stick) in pyraziflumid, prolonged amide bond (gray and yellow stick) in pydiflumetofen and fluopyram, and diphenyl-ether (magenta stick) in flubeneteram. (E) Binding mode of compound **6y** with SDH. (F) Overlay of pyraziflumid (yellow stick) and **6y** (magenta stick) when bound with SDH. Only the key residues are shown. The red and green lines represent an Hbond. All these figures were built by a Pymol program.

RESULTS AND DISCUSSION

Fragment Identification and Recombination. Finding novel fragments as starting points for optimization is a major challenge in FBDD. The structures of the fragments binding to the protein can be used to design new compounds with increased affinity and novelty. The chemical structure of commercial SDH fungicides always consists of three fragments, including an acid moiety, hydrophobic side moiety, and amide linker, indicating three fragment directions for designing novel SDHI.[21,38] According to our previous study, an acid moiety bound to the bottom of the SDH binding site formed a cation−π interaction with C_R46, an amide linker located at the mouth of the SDH binding site formed a hydrogen bond (Hbond) with B_W173 and D_Y91, and a hydrophobic side moiety extended outside of the SDH binding site formed hydrophobic interaction with some residues, such as C_W35, D_Y91, and C_I30, among others (Figure 1S, Supporting Information).[30]

Some active fragments from commercial fungicides are good choices for designing SDHIs. The pyrazine-carboxamide fungicide pyraziflumid with structural novelty was developed by Nihon Nohyaku Co., Ltd. in 2017 with excellent biological performance and no cross resistance with the existing fungicides.[39] The main difference between pyraziflumid and other SDH fungicides is its pyrazine ring in the acid moiety. Understanding the binding mechanism of these highly potent inhibitors can help to uncover the binding "hot spots" and identify the regions contributing to activity. Hence, molecular docking followed by molecular dynamics and MM/PBSA calculations was performed for pyraziflumid. As shown in Figure 2A, pyraziflumid showed a conserved binding mode with other carboxamide SDH fungicides. The pyrazine ring in pyraziflumid, similar to other acid moieties in SDHIs, bound to the bottom of the SDH binding site and formed a cation−π interaction with the residue of C_R46. The carbonyl oxygen in pyraziflumid formed an Hbond with D_Y91 and B_W173, its biphenyl moiety extended toward the entrance of the SDH binding site, then its inner phenyl bounded by C_I30, C_I43, and C_W35, and its tail phenyl formed the edge-to-edge $\pi-\pi$ interaction with D_Y91. Here, we noticed that the ring plane of inner phenyl in pyraziflumid was misaligned with C_I30 and C_W35 (Figure 2B), which could be further structurally optimized to increase its activity. Collectively, these results indicated that a pyrazine ring as an acid moiety would be a good starting point to design new SDHIs.

Moreover, in our previous study, the diphenyl-ether in flubeneteram was proven as a good fragment extending toward the entrance of the SDH binding site, forming a T−π interaction with the indole ring of C_W35.[24,40] To continue our research, the diphenyl-ether was selected as the hydrophobic side fragment in this work. Here, we noticed that the distance between the pyrazine ring and diphenyl-ether in the SDH binding site was about 5.1 Å, which was larger than one amide bond length (3.8 Å) (Figure 2S, Supporting Information).

For the linker between the pyrazine ring and diphenyl-ether, the prolonged amide bond with one or two methylene groups

https://dx.doi.org/10.1021/acs.jafc.0c05646
J. Agric. Food Chem. XXXX, XXX, XXX−XXX

Scheme 1. Synthetic Route for the Target Compounds 6a−6z[a]

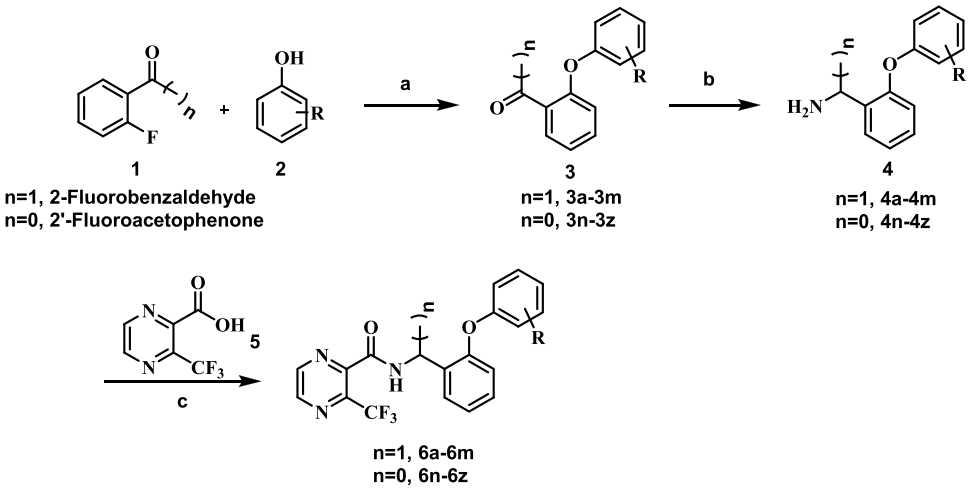

[a]Reagents and conditions: (a) K_2CO_3, DMF, reflux; (b) $NH_2OH{\cdot}HCl$, EtOH, reflux; Zn/HCl, room temperature; (c) **5**, HATU/DIPEA, CH_2Cl_2, room temperature.

Table 1. Chemical Structures, Inhibitory Activities against Porcine SDH, and the Binding Energy between Compounds with SDH (kcal/mol)

no.	*n*	R	inhibitory rate (%)/IC_{50} (μM)[a]	ΔE_{vdw}	ΔE_{ele}	ΔG_{pol}	ΔG_{np}	ΔG_{cal}	ΔG_{exp}
6a	1	2-F	23.61%	[b]					
6b	1	2-Br	48.43%						
6c	1	2-Me	29.27%						
6d	1	3-Cl	31.42%						
6e	1	4-Me	32.45%						
6f	1	4-Br	32.85%						
6g	1	2,3-F_2	26.16%						
6h	1	2,3-Cl_2	59.68%						
6i	1	2-Cl-4-F	54.83%						
6g	1	2,4-Cl_2	43.27%						
6k	1	2-Cl-4-CF_3	63.37%	−36.44	−24.27	45.12	−3.80	−19.39	
6l	1	3,4-F_2	31.34%						
6m	1	3,4-Cl_2	52.45%						
6n	0	2-F	4.79 ± 0.12	−39.86	−19.45	37.98	−3.85	−25.19	−7.30
6o	0	2-Cl	1.25 ± 0.12	−40.83	−20.55	36.78	−3.82	−28.42	−8.10
6p	0	2-Br	3.04 ± 0.01	−40.99	−18.91	37.77	−3.86	−25.99	−7.57
6q	0	4-F	5.40 ± 0.12	−39.92	−17.67	36.17	−3.60	−25.01	−7.23
6r	0	2,3-F_2	3.40 ± 0.01	−40.62	−22.59	40.59	−3.84	−26.45	−7.50
6s	0	2-Cl-3-F	2.72 ± 0.12	−40.42	−20.94	37.63	−3.62	−27.34	−7.64
6t	0	2,3-Cl_2	0.90 ± 0.01	−42.40	−17.70	34.12	−3.78	−29.76	−8.30
6u	0	3,4-F_2	4.18 ± 0.11	−40.31	−20.25	38.49	−3.78	−25.85	−7.38
6v	0	2,4-Cl_2	1.14 ± 0.12	−40.44	−20.63	36.02	−3.72	−28.77	−8.15
6w	0	2-Cl-4-F	2.67 ± 0.11	−38.30	−18.39	33.03	−3.43	−27.08	−7.65
6x	0	2-Cl-4-CF_3	1.23 ± 0.12	−41.73	−16.59	33.65	−3.75	−28.42	−8.11
6y	0	2-Br-4-Cl	0.83 ± 0.01	−45.88	−19.80	38.80	−3.94	−30.83	−8.34
6z	0	2-Cl-5-F	3.49 ± 0.12	−40.01	−18.59	36.01	−3.57	−26.16	−7.49
pyraziflumid			1.52 ± 0.11	−41.68	−19.77	36.57	−3.49	−28.37	−7.98

[a]The compound inhibitory rate was first tested at 10 μM concentration. If the inhibitory rate was over 70%, then the IC_{50} value would be calculated with eight different concentration gradients. [b]Not tested.

was taken into consideration. Here, the commercial fungicides, pydiflumetofen and fluopyram, with different novel prolonged strategies for the amide bond (Figure 1), were selected as representative compounds to study the interaction with the target SDH.[41,42] As shown in Figure 3S (Supporting Information), both of them formed an Hbond with B_W173 and D_Y91 and a cation−π interaction with C_R46. Compared to the classical amide bond linker, the N-alkyl amide linker in pydiflumetofen is also located at the mouth of the SDH binding site, and then the difference was that the prolonged amide linker in pydiflumetofen resulted in its substituted phenyl ring extending further outside of the binding site to form $\pi-\pi$ interaction with C_W35 rather than pyraziflumid (Figure 2C). The same thing occurred to the ethanamine linker in fluopyram (Figure 2C). These results indicated that the prolonged amide bond could adjust the

https://dx.doi.org/10.1021/acs.jafc.0c05646
J. Agric. Food Chem. XXXX, XXX, XXX−XXX

interaction of the hydrophobic side moiety as an inhibitor with SDH. Our previous study showed that as more interaction occurs between the hydrophobic side moiety in the inhibitor and SDH, the stronger the activity of the inhibitor.[32]

Subsequently, four virtual compounds (virtual-1, virtual-2, virtual-3, and virtual-4) were designed based on the relative position of the pyrazine ring, diphenyl-ether, and prolonged amide bond in the SDH binding site (Figure 2D). Then, four of them were docked to the SDH binding site. As shown in Figure 4S, the ring plane of the pyrazine fragment in virtual-1 did not form a good cation−π interaction with C_R46, and virtual-2 just formed one Hbond with B_W173. However, virtual-3 and virtual-4 showed the conserved binding modes with that of the commercial fungicides, indicating that they could be selected as the new starting points for SDHIs and subjected to subsequent synthesis. Meanwhile, the synthesis processes of virtual-3 and virtual-4 were simpler than those of virtual-1 and virtual-2 as described in the following Chemistry section.

Chemistry. To enrich the structural−activity relationship (SAR) of virtual-3 (equal to **6k**) and virtual-4 (equal to **6x**), a series of pyrazine-carboxamide-diphenyl-ether compounds (**6a**−**6z**) were synthesized. According to Scheme 1, compounds **6a**−**6m** were synthesized with yields of 37−66% by only three steps. The substituted phenol **2** and 2′-fluoroacetophenone **1** were selected as the starting materials and then employed under the presence of K_2CO_3 in DMF to produce intermediate **3**.[43] Intermediate **3** reacted with $NH_2OH{\cdot}HCl$ to afford oxime and then was restored to key intermediate amine **4** under a zinc duct.[44] Finally, compound **5**, 3-(trifluoromethyl)pyrazine-2-carboxylic acid, was obtained according to reported methods[39] and then reacted with amine **4** to afford the target compounds **6a**−**6m** by the condensing agent HATU/DIPEA catalyst. The compounds **6n**−**6z** were synthesized with 2-fluorobenzaldehyde as a starting material, and their yields were about 32−62%.

Structural−Activity Relationship. As shown in Table 1, **6a**−**6m** showed weak enzymatic inhibition activity with an inhibitory rate ranging from 23.61 to 63.37% against porcine SDH at 10 μM. To understand its low activity, compound **6k** was redocked followed by MM/PBSA calculations. The binding energy with SDH was −19.39 kcal/mol, which was larger than the binding energy of pyraziflumid with SDH (−28.37 kcal/mol). Here, we noticed that the VDW interaction energy of **6k** with SDH was −36.44 kcal/mol (Table 1), which was lower than pyraziflumid (−41.68 kcal/mol) and may explain its low activity.

However, the activity of compounds **6n**−**6z** showed significant improvement over **6a**−**6m.** Moreover, the IC_{50} values of compounds **6o**, **6t**, **6v**, and **6x** were 1.25, 0.90, 1.14, and 1.23 μM, respectively, which showed higher activities than pyraziflumid (IC_{50} = 1.52 μM). Remarkably, compound **6y**, bearing 2-Br-4-Cl, displayed the highest activity with an IC_{50} value of 0.83 μM, with approximately 2-fold improved potency compared with pyraziflumid. The SARs of compounds **6n**−**6z** are summarized as follows: (1) Monosubstituted compounds, a 2-position substituent, had a positive effect on the activities compared to a 4-position substituent. For example, **6n** (2-F, IC_{50} = 4.79 μM) showed a higher activity than **6q** (4-F, IC_{50} = 5.40 μM). (2) Disubstituted compounds always had better activity than monosubstituted compounds. (3) For 2,4-disubstituted compounds, **6v** showed a higher activity (2,4-Cl_2, IC_{50} = 1.14 μM) than **6x** (2-Cl-4-CF_3, IC_{50} = 1.23 μM) and **6w** (2-Cl-4-F, IC_{50} = 2.67 μM).

To further understand SAR, molecular docking was used to explore the inhibition mechanism of compounds **6n**−**6z**. As shown in Table 1, the correlation coefficient (R^2) between ΔG_{cal} (calculated binding energies) and ΔG_{exp} ($\Delta G_{exp} = -RT \times \ln IC_{50}$) was high, up to 0.95, which indicated that the binding mode was reasonable and reliable. The binding mode of the representative compound **6y** (Figure 2E) was similar to pyraziflumid, forming a cation−π interaction with C_R46 and a Hbond with B_W173 and D_Y91. The pyrazine ring in **6y** showed nearly the same position as that in pyraziflumid. Different from pyraziflumid (Figure 2F), the amide bond extension in **6y** led to its diphenyl-ether moiety extending toward the binding site entrance of SDH, forming a stronger sandwich hydrophobic interaction with C_I30 and C_I43 than pyraziflumid (Figure 2F). This resulted in a more favorable VDW interaction with SDH (ΔE_{vdw} = −45.88 kcal/mol for compound **6y** vs −41.68 kcal/mol for pyraziflumid, Table 1). Then, we also noticed that the ΔE_{vdw} values for compounds **6n**−**6z** were around −38.30 to −42.40 kcal/mol, lower than **6k** (−36.44 kcal/mol), indicating that one methyl introduction (n = 1) into the scaffold of the target was unfavorable for VDW interaction between the ligand and SDH.

As shown in Table 1, one interesting thing was that the increase in ΔE_{ele} was not able to enhance the activity of the compound. For example, compound **6r** had the highest ΔE_{ele} (−22.59 kcal/mol) but its IC_{50} value (3.40 μM) was not good. However, the influence of ΔE_{vdw} was remarkable. In general, the stronger the ΔE_{vdw} between the compound and SDH, the higher the activity of the compound, such as in compounds **6t**, **6k**, and **6y**. These results indicated that ΔE_{vdw} is very important for designing new SDH inhibitors.

We note that the activity of compound **6y** was still lower than pydiflumetofen (0.13 μM, data was not shown) and flubeneteram (0.11 μM). Nevertheless, the scaffold of compound **6y**, especially for its amide bond with one methylene extension, provides new insight into designing new SDHIs.

***In Vitro* Fungicidal Activity.** To determine whether the target compounds had fungicidal activity, compounds **6n**−**6z** were assessed on six plant pathogens, namely, *Ph. capsici*, *Py. dissimile*, *B. fuckeliana*, *G. zeae*, *Z. tritici*, and *U. viciae-fabae*. The results are summarized in Table 2 and expressed as general assessment criteria for biological assays.

As shown in Table 2, all tested compounds did not show good fungicidal activity against *Ph. capsici*, *Py. dissimile*, *G. zeae*, *Z. tritici*, and *U. viciae-fabae*. In contrast, most compounds showed an over 80% inhibitory rate activity against *B. fuckeliana*, except **6x**, with a 62% inhibitory rate at 20 mg/L. Furthermore, compounds **6o**−**6r**, **6u**, **6y**, and **6z** had a 100% control effect against *B. fuckeliana*, which was better than pyraziflumid (90%). Compound **6y** also showed an 80% inhibitory rate against *Z. tritici* at a concentration of 20 mg/L, indicating its potential broad-spectrum property.

***In Vivo* Fungicidal Activities.** It is known that gray mold caused by *B. fuckeliana* can cause heavy losses in many crop yields worldwide, such as grapes, soybean, cucumber, and strawberry.[45] Here, soybean gray mold (SGM) and wheat powdery mildew (WPM) were selected as the target diseases to evaluate the biological activity of the tested compounds in the greenhouse, and the commercial fungicide pyraziflumid was selected as a positive control. As shown in Table 3, most

https://dx.doi.org/10.1021/acs.jafc.0c05646
J. Agric. Food Chem. XXXX, XXX, XXX−XXX

Table 2. Fungicidal Activity of Target Compounds *In Vitro*

no.	Uvf[a] 100[b]	Pd[a] 2[b]	Bf[a] 20[b]	Gz[a] 20[b]	Pc[a] 20[b]	Zt[a] 20[b]
6n	0[c]	0	95 ± 1	0	0	0
6o	0	0	100	0	0	0
6p	0	0	100	0	0	0
6q	0	0	100	0	0	0
6r	0	0	100	0	0	0
6s	0	0	90 ± 1	0	0	0
6t	0	0	85 ± 2	0	0	0
6u	0	0	100	0	0	27 ± 2
6v	0	0	90 ± 1	0	0	0
6w	0	0	80 ± 2	0	0	0
6x	0	0	62 ± 1	0	0	0
6y	0	0	100	0	0	80 ± 1
6z	0	0	100	0	0	0
pyraziflumid	100	0	90 ± 1	0	0	0
azoxystrobin	100	100	100	0	100	100
prochloraz	0	0	100	100	0	100

[a]Uvf, *U. viciae-fabae*; Pd, *Py. dissimile*; Bf, *B. fuckeliana*; Gz, *G. zeae*; Pc, *Ph. capsici*; Zt, *Z. tritici*. [b]Dose in mg/L. [c]The data are the mean of three replicates.

compounds did not show good activity against WPM. As expected, for SGM at 100 mg/L, compounds **6p**, **6r**, **6u**, and **6z** showed over a 80% control effect, and compounds **6o**, **6q**, and **6y** showed over a 90% control effect, all of which were better than pyraziflumid (70%). Notably, compound **6y** had a 95% control effect against SGM and an 80% control effect against WPM at a concentration of 100 mg/L. Compound **6q** had nearly the same control effect against SGM and WPM as **6y.** Then, the EC_{50} and EC_{90} were tested against SGM for some potential compounds. The results are shown in Table 4 (Table 1S, Supporting Information), and we can see that compounds **6y** and **6q** exhibited better EC_{50} and EC_{90} values than pyraziflumid. These results indicated that compounds **6y** and **6q** have potential broad-spectrum features and thus may be used as candidates for further development.

In summary, we implemented a fragment recombination strategy for new SDHI design. Computational analysis demonstrates that three active fragments, pyrazine ring, diphenyl-ether, and prolonged amide bond, occupied three different sub-pockets in the SDH binding site and could be combined to a novel scaffold of SDHI. After substitute optimizations, a hit compound **6y**, *N*-(2-(2-bromo-4-chlorophenoxy)benzyl)-3-(trifluoromethyl)pyrazine-2-carboxamide, was identified with an IC_{50} value 0.83 μM, which was about 2-fold more potent than pyraziflumid. Biological experiments showed that compounds **6q** and **6y** had 100% control effects against *B. fuckeliana* at a dosage of 20 mg/L *in vitro* and over 90% control effects against SGM at 100 mg/L *in vivo*, which were also better than that of pyraziflumid. Further EC_{50} and EC_{90} values also indicated that both of them were superior to pyraziflumid. The computational simulations revealed that the van der Waals interactions between compounds and SDH played an important role in adjusting its activity, which may provide insight into designing new SDHIs. The above results also indicated that the amide bond with one methylene extension is a novel active fragment for designing SDHIs.

Table 4. EC_{50} and EC_{90} Values (mg/L) for Target Compounds against Soybean Gray Mold

no.	EC_{50}	EC_{90}	regression equation	r
6p	76.51	139.74	−4.2278 + 4.8987*x*	0.94
6o	72.04	128.97	−4.4124 + 5.0671*x*	0.95
6y	52.28	87.61	−4.8227 + 5.7163*x*	0.93
6q	57.24	96.90	−4.8523 + 5.6052*x*	0.94
pyraziflumid	60.96	107.06	−4.3515 + 5.2389*x*	0.91

ASSOCIATED CONTENT

Supporting Information

The Supporting Information is available free of charge at https://pubs.acs.org/doi/10.1021/acs.jafc.0c05646.

Relative position, binding mode, decomposed VDW interaction energy, control effect picture, enzymatic assay, *in vitro* and *in vivo* fungicidal assay, leaf-piece assay, synthetic routes, and ^{1}H and ^{13}C NMR spectrograms (PDF)

AUTHOR INFORMATION

Corresponding Authors

Xiao-Lei Zhu − *Key Laboratory of Pesticide & Chemical Biology of Ministry of Education, International Joint Research Center for Intelligent Biosensor Technology and Health of Ministry of Science and Technology, Central China Normal University, Wuhan 430079, People's Republic of China;* orcid.org/0000-0002-5672-5209; Email: xlzhu@mail.ccnu.edu.cn

Guang-Fu Yang − *Key Laboratory of Pesticide & Chemical Biology of Ministry of Education, International Joint Research Center for Intelligent Biosensor Technology and Health of Ministry of Science and Technology, Central China Normal University, Wuhan 430079, People's Republic of China; Collaborative Innovation Center of Chemical Science and Engineering, Tianjin 300071, People's Republic of China;* Phone: 86-27-67867800; Email: gfyang@mail.ccnu.edu.cn; Fax: 86-27-67867141

Table 3. Fungicidal Activity of Target Compounds *In Vivo*

no.	SGM[a] (100 mg/L)	WPM[a] (100 mg/L)	no.	SGM[a] (100 mg/L)	WPM[a] (100 mg/L)
6n	0	NT[b]	**6u**	80	20
6o	90	30	**6v**	0	NT
6p	85	40	**6w**	20	NT
6q	90	85	**6x**	10	NT
6r	85	30	**6y**	95	80
6s	20	NT	**6z**	80	0
6t	0	NT	pyraziflumid	70	98

[a]SGM, soybean gray mold; WPM, wheat powdery mildew. [b]Not tested.

https://dx.doi.org/10.1021/acs.jafc.0c05646
J. Agric. Food Chem. XXXX, XXX, XXX−XXX

Authors

Hua Li − *Key Laboratory of Pesticide & Chemical Biology of Ministry of Education, International Joint Research Center for Intelligent Biosensor Technology and Health of Ministry of Science and Technology, Central China Normal University, Wuhan 430079, People's Republic of China*

Meng-Qi Gao − *Key Laboratory of Pesticide & Chemical Biology of Ministry of Education, International Joint Research Center for Intelligent Biosensor Technology and Health of Ministry of Science and Technology, Central China Normal University, Wuhan 430079, People's Republic of China*

Yan Chen − *Key Laboratory of Pesticide & Chemical Biology of Ministry of Education, International Joint Research Center for Intelligent Biosensor Technology and Health of Ministry of Science and Technology, Central China Normal University, Wuhan 430079, People's Republic of China*

Yu-Xia Wang − *Key Laboratory of Pesticide & Chemical Biology of Ministry of Education, International Joint Research Center for Intelligent Biosensor Technology and Health of Ministry of Science and Technology, Central China Normal University, Wuhan 430079, People's Republic of China*

Complete contact information is available at: https://pubs.acs.org/10.1021/acs.jafc.0c05646

Funding

The research was supported in part by the National Key Research and Development Program of China (2018YFD0200100), the Key Research and Development Program of Hubei Province (2020BBA052), and the National Natural Science Foundation of China (no.21977035, 21837001, and 21772057).

Notes

The authors declare no competing financial interest.

■ ACKNOWLEDGMENTS

This paper is dedicated to Professor Youyou Tu, the 2015 Nobel Prize Laureate of Physiology or Medicine, on the occasion of her 90th birthday.

■ REFERENCES

(1) Cecchini, G. Function and structure of complex II of the respiratory chain. *Annu. Rev. Biochem.* **2003**, *72*, 77−109.

(2) Sun, F.; Huo, X.; Zhai, Y.; Wang, A.; Xu, J.; Su, D.; Bartlam, M.; Rao, Z. Crystal structure of mitochondrial respiratory membrane protein complex II. *Cell* **2005**, *121*, 1043−1057.

(3) Maklashina, E.; Cecchini, G. The quinone-binding and catalytic site of complex II. *Biochim. Biophys. Acta* **1797**, *1797*, 1877−1882.

(4) Yankovskaya, V.; Horsefield, R.; Törnroth, S.; Luna-Chavez, C.; Miyoshi, H.; Leger, C.; Byrne, B.; Cecchini, G.; Iwata, S. Architecture of succinate dehydrogenase and reactive oxygen species generation. *Science* **2003**, *299*, 700−704.

(5) Ralph, S. J.; Moreno-Sánchez, R.; Neuzil, J.; Rodríguez-Enríquez, S. Inhibitors of succinate: Quinone reductase/Complex II regulate production of mitochondrial reactive oxygen species and protect normal cells from ischemic damage but induce specific cancer cell death. *Pharm. Res.* **2011**, *28*, 2695−2730.

(6) Keohane, C. E.; Steele, A. D.; Fetzer, C.; Khowsathit, J.; Van Tyne, D.; Moynié, L.; Gilmore, M. S.; Karanicolas, J.; Sieber, S. A.; Wuest, W. M. Promysalin elicits species-selective inhibition of *Pseudomonas aeruginosa* by targeting succinate dehydrogenase. *J. Am. Chem. Soc.* **2018**, *140*, 1774−1782.

(7) FRAC(Fungicide Resistance Action Committee) *Code List 2019, fungicides sorted by mode of action*; www.frac,info. (accessed Aug 10, 2019)

(8) Avenot, H. F.; Sellam, A.; Karaoglanidis, G.; Michailides, T. J. Characterization of mutations in the iron-sulphur subunit of succinate dehydrogenase correlating with *Boscalid* resistance in *Alternaria alternata* from California pistachio. *Phytopathology* **2008**, *98*, 736−742.

(9) Mallik, I.; Arabiat, S.; Pasche, J. S.; Bolton, M. D.; Patel, J. S.; Gudmestad, N. C. Molecular characterization and detection of mutations associated with resistance to succinate dehydrogenase-inhibiting fungicides in *Alternaria solani*. *Phytopathology* **2014**, *104*, 40−49.

(10) Rehfus, A.; Strobel, D.; Bryson, R.; Stammler, G. Mutations in sdh genes in field isolates of *Zymoseptoria tritici* and impact on the sensitivity to various succinate dehydrogenase inhibitors. *Plant Pathol.* **2018**, *67*, 175−180.

(11) Hao, G.-F.; Jiang, W.; Ye, Y.-N.; Wu, F.-X.; Zhu, X.-L.; Guo, F.-B.; Yang, G.-F. ACFIS: A web server for fragment-based drug discovery. *Nucleic Acids Res.* **2016**, *44*, 550−556.

(12) Lin, H.-Y.; Chen, X.; Chen, J.-N.; Wang, D.-W.; Wu, F.-X.; Lin, S.-Y.; Zhan, C.-G.; Wu, J.-W.; Yang, W.-C.; Yang, G.-F. Crystal structure of 4-hydroxyphenylpyruvate dioxygenase in complex with substrate reveals a new starting point for herbicide discovery. *Research* **2019**, *2019*, 2602414.

(13) Wang, F.; Yang, J.-F.; Wang, M.-Y.; Jia, C.-Y.; Shi, X.-X.; Hao, G. -F.; Yang, G.-F. Graph attention convolutional neural network model for chemical poisoning of honey bees' prediction. *Sci. Bull.* **2020**, *65*, 1184−1191.

(14) Wu, F.-X.; Wang, F.; Yang, J.-F.; Jiang, W.; Wang, M.-Y.; Jia, C.-Y.; Hao, G.-F.; Yang, G.-F. AIMMS suite: A web server dedicated for prediction of drug resistance on protein mutation. *Briefings Bioinf.* **2020**, *20*, 318−328.

(15) Kumar, A.; Voet, A.; Zhang, K. Y. J. Fragment based drug design: From experimental to computational approaches. *Curr. Med. Chem.* **2012**, *19*, 5128−5147.

(16) Mondal, M.; Radeva, N.; Fanlo-Virgós, H.; Otto, S.; Klebe, G.; Hirsch, A. K. H. Fragment linking and optimization of inhibitors of the aspartic protease endothiapepsin: Fragment-based drug design facilitated by dynamic combinatorial chemistry. *Angew. Chem., Int. Ed.* **2016**, *55*, 9422−9426.

(17) Erlanson, D. A.; de Esch, I. J. P.; Jahnke, W.; Johnson, C. N.; Mortenson, P. N. Fragment-to-lead medicinal chemistry publications in 2018. *J. Med. Chem.* **2020**, *63*, 4430−4444.

(18) Mortenson, P. N.; Erlanson, D. A.; de Esch, I. J. P.; Jahnke, W.; Johnson, C. N. Fragment-to-lead medicinal chemistry publications in 2017. *J. Med. Chem.* **2019**, *62*, 3857−3872.

(19) Barelier, S.; Pons, J.; Marcillat, O.; Lancelin, J. M.; Krimm, I. Fragment-based deconstruction of Bcl-xL inhibitors. *J. Med. Chem.* **2010**, *53*, 2577−2588.

(20) Bancet, A.; Raingeval, C.; Lomberget, T.; Le Borgne, M.; Guichou, J.-F.; Krimm, I. Fragment linking strategies for structure-based drug design. *J. Med. Chem.* **2020**, *63*, 11420.

(21) Yang, D.; Zhao, B.; Fan, Z.; Yu, B.; Zhang, N.; Li, Z.; Zhu, Y.; Zhou, J.; Kalinina, T. A.; Glukhareva, T. V. Synthesis and biological activity of novel succinate dehydrogenase inhibitor derivatives as potent fungicide candidates. *J. Agric. Food Chem.* **2019**, *67*, 13185−13194.

(22) Hao, G.-F.; Zuo, Y.; Yang, S.-G.; Chen, Q.; Zhang, Y.; Yin, C.-Y.; Niu, C.-W.; Xi, Z.; Yang, G.-F. Computational discovery of potent and bioselective protoporphyrinogen IX oxidase inhibitor via fragment deconstruction analysis. *J. Agric. Food Chem.* **2017**, *65*, 5581−5588.

(23) Hao, G.-F.; Wang, F.; Li, H.; Zhu, X.-L.; Yang, W.-C.; Huang, L.-S.; Wu, J.-W.; Berry, E.-A.; Yang, G.-F. Computational discovery of picomolar Q(o) site inhibitors of cytochrome bc_1 complex. *J. Am. Chem. Soc.* **2012**, *134*, 11168−11176.

(24) Xiong, L.; Li, H.; Jiang, L.-N.; Ge, J.-M.; Yang, W.-C.; Zhu, X.-L.; Yang, G.-F. Structure-based discovery of potential fungicides as succinate ubiquinone oxidoreductase inhibitors. *J. Agric. Food Chem.* **2017**, *65*, 1021−1029.

(25) Howard, N.; Abell, C.; Blakemore, W.; Chessari, G.; Congreve, M.; Howard, S.; Jhoti, H.; Murray, C. W.; Seavers, L. C. A.; van Montfort, R. L. Application of fragment screening and fragment linking to the discovery of novel thrombin inhibitors. *J. Med. Chem.* **2006**, *49*, 1346−1355.
(26) Zhu, X.-L.; Zhang, R.; Wu, Q.-Y.; Song, Y.-J.; Wang, Y.-X.; Yang, J.-F.; Yang, G.-F. Natural product neopeltolide as a cytochrome bc_1 complex inhibitor: Mechanism of action and structural modification. *J. Agric. Food Chem.* **2019**, *67*, 2774−2781.
(27) Morris, G. M.; Goodsell, D. S.; Halliday, R. S.; Huey, R.; Hart, W. E.; Belew, R. K.; Olson, A. J. Automated docking using a Lamarckian genetic algorithm and an empirical binding free energy function. *J. Comput. Chem.* **1998**, *19*, 1639−1662.
(28) Case, D. A. *AMBER 16*; University of California: San Francisco, CA, 2016.
(29) Hornak, V.; Abel, R.; Okur, A.; Strockbine, B.; Roitberg, A.; Simmerling, C. Comparison of multiple Amber force fields and development of improved protein backbone parameters. *Proteins* **2006**, *65*, 712−725.
(30) Zhu, X.-L.; Xiong, L.; Li, H.; Song, X.-Y.; Liu, J.-J.; Yang, G.-F. Computational and experimental insight into the molecular mechanism of carboxamide inhibitors of succinate-ubquinone oxidoreductase. *ChemMedChem* **2014**, *9*, 1512−1521.
(31) King, T. E. Preparations of succinate—cytochrome c reductase and the cytochrome bc_1 particle, and reconstitution of succinate-cytochrome c reductase. *Methods Enzymol.* **1967**, *10*, 216−225.
(32) Fisher, N.; Bourges, I.; Hill, P.; Brasseur, G.; Meunier, B. Disruption of the interaction between the Rieske iron-sulfur protein and cytochrome b in the yeast bc1 complex owing to a human disease-associated mutation within cytochrome b. *Eur. J. Biochem.* **2004**, *271*, 1292−1298.
(33) Xiong, L.; Zhu, X.-L.; Shen, Y.-Q.; Wishwajith, W. K. W. M.; Li, K.; Yang, G.-F. Discovery of N-benzoxazol-5-yl-pyrazole-4-carboxamides as nanomolar SQR inhibitors. *Eur. J. Med. Chem.* **2015**, *95*, 424−434.
(34) Cheng, H.; Shen, Y. Q.; Pan, X. Y.; Hou, Y. P.; Wu, Q. Y.; Yang, G. F. Discovery of 1,2,4-triazole-1,3-disulfonamides as dual inhibitors of mitochondrial complex II and complex III. *New J. Chem.* **2015**, *39*, 7281−7292.
(35) Lin, L.; Mulholland, N.; Huang, S. W.; Beattie, D.; Irwin, D.; Gu, Y. C.; Clough, J.; Wu, Q. Y.; Yang, G. F. Design, synthesis and fungicidal activity of novel sclerotiorin derivatives. *Chem. Biol. Drug Des.* **2012**, *80*, 682−692.
(36) Zhang, M. Z.; Jia, C. Y.; Gu, Y. C.; Mulholland, N.; Turner, S.; Beattie, D.; Zhang, W. H.; Yang, G. F.; Clough, J. Synthesis and antifungal activity of novel indole-replaced streptochlorin analogues. *Eur. J. Med. Chem.* **2017**, *126*, 669−674.
(37) Guan, A.; Liu, C.; Chen, W.; Yang, F.; Xie, Y.; Zhang, J.; Li, Z.; Wang, M. Design, synthesis, and structure-activity relationship of new pyrimidinamine derivatives containing an aryloxy pyridine moiety. *J. Agric. Food Chem.* **2017**, *65*, 1272−1280.
(38) Yu, B.; Zhou, S.; Cao, L.; Hao, Z.; Yang, D.; Guo, X.; Zhang, N.; Bakulev, V. A.; Fan, Z. Design, synthesis, and evaluation of the antifungal activity of novel pyrazole-thiazole carboxamides as succinate dehydrogenase inhibitors. *J. Agric. Food Chem.* **2020**, *68*, 7093.
(39) Oda, M.; Furuya, T.; Morishita, Y.; Matsuzaki, Y.; Hasebe, M.; Kuroki, N. Synthesis and biological activity of a novel fungicide, pyraziflumid. *J. Pestic. Sci.* **2017**, *42*, 151−157.
(40) Chen, T.; Xiong, H.; Yang, J.-F.; Zhu, X.-L.; Qu, R.-Y.; Yang, G. F. Diaryl ether: A Privileged scaffold for drug and agrochemical discovery. *J. Agric. Food Chem.* **2020**, *68*, 9839.
(41) Sun, H. Y.; Cui, J. H.; Tian, B. H.; Cao, S. L.; Zhang, X. X.; Chen, H. G. Resistance risk assessment for *Fusarium graminearum* to pydiflumetofen, a new succinate dehydrogenase inhibitor. *Pest Manage. Sci.* **2020**, *76*, 1549−1559.
(42) Veloukas, T.; Karaoglanidis, G. S. Biological activity of the succinate dehydrogenase inhibitor fluopyram against *Botrytis cinerea* and fungal baseline sensitivity. *Pest Manage. Sci.* **2012**, *68*, 858−864.
(43) Harris, T. W.; Smith, H. E.; Mobley, P. L.; Manier, D. H.; Sulser, F. Affinity of 10-(4-methylpiperazino) dibenz [b,f] oxepins for clozapine and spiroperidol binding sites in rat brain. *J. Med. Chem.* **1982**, *25*, 855−858.
(44) Ayedi, M. A.; Le Bigot, Y.; Ammar, H.; Abid, S.; Gharbi, R. E.; Delmas, M. Synthesis of primary amines by one-Pot reductive amination of aldehydes. *Synth. Commun.* **2013**, *43*, 2127−2133.
(45) Lane, A.; Gladders, P. Pests and diseases of oilseeds, brassica seed crops and field beans. In *Pest and Disease Management Handbook*; Alford, D. V., Ed.; John Wiley: New York, 2000; 52−83.

https://dx.doi.org/10.1021/acs.jafc.0c05646
J. Agric. Food Chem. XXXX, XXX, XXX−XXX